

# Spatial patterns of competing random walkers

Emilio Hernández-García<sup>a</sup>, Els Heinsalu<sup>b,c</sup>, Cristóbal López<sup>a</sup>

<sup>a</sup>*IFISC (CSIC-UIB) Instituto de Física Interdisciplinar y Sistemas Complejos, Campus Universitat de les Illes Balears, E-07122 Palma de Mallorca, Spain*

<sup>b</sup>*Niels Bohr International Academy, Niels Bohr Institute, Blegdamsvej 17, DK-2100 Copenhagen, Denmark*

<sup>c</sup>*National Institute of Chemical Physics and Biophysics, Rāvala 10, 15042 Tallinn, Estonia*

---

## Abstract

We review recent results obtained from simple individual-based models of biological competition in which birth and death rates of an organism depend on the presence of other competing organisms close to it. In addition the individuals perform random walks of different types (Gaussian diffusion and Lévy flights). We focus on how competition and random motions affect each other, from which spatial instabilities and extinctions arise. Under suitable conditions, competitive interactions lead to clustering of individuals and periodic pattern formation. Random motion has a homogenizing effect and then delays this clustering instability. When individuals from species differing in their random walk characteristics are allowed to compete together, the ones with a tendency to form narrower clusters get a competitive advantage over the others. Mean-field deterministic equations are analyzed and compared with the outcome of the individual-based simulations.

*Keywords:* Competition, Clustering, Pattern formation, Individual-based model, Nonlocal interactions, Niche space, Random walks, Lévy flights

---

## 1. Introduction

Competitive interactions are among the basic building blocks shaping ecosystems and driving evolution. In its basic form, competition refers to the situation in which two organisms utilize the same resource to survive and

---

*Email address:* [emilio@ifisc.uib-csic.es](mailto:emilio@ifisc.uib-csic.es) (Emilio Hernández-García)

grow. If one of them consumes the resource, it is no longer available for the other, which will then experience a decrease in growth capacity, increase of mortality, or both. This basic effect of competition as a limitation to growth is already present in very early population dynamics mathematical models such as the Verhulst or logistic equation (Ausloos and Dirickx, 2006), or in its simplest generalization when taking into account spatial dispersion, the Fisher or Fisher-Kolmogorov-Petrovskii-Piskunov (FKPP) partial differential equation (Okubo and Levin, 2001; Murray, 2002; Méndez et al., 2014). Resource limitation in such models defines a carrying capacity which becomes the stable asymptotic value of the population density. When space is taken into account, this stable state advances into unpopulated regions as a propagating front (Fife, 1979; Okubo and Levin, 2001; Murray, 2002; Méndez et al., 2014).

It was recognized some time ago (Britton, 1989; Sasaki, 1997) that, in this situation in which the spatial dimension is considered, the competition spatial range is an important parameter than can change qualitatively population dynamics. In particular, population density can arrange into spatially periodic patterns when competitive interactions occur within a finite region around the individuals (Britton, 1989; Sasaki, 1997). This is in contrast with the homogeneous configurations attained from the FKPP model that assumes a strictly local competition. In these works the finite range of interaction enters the description via an integral term, converting the FKPP model into an integrodifferential equation, the nonlocal FKPP model. In this mathematical framework, the problem of individuals or populations competing for resources in space becomes formally identical to the one of different species (MacArthur and Levins, 1967), or even different phenotypes of the same species (Roughgarden, 1979, p. 534), competing for resources distributed in the so-called *niche space*. This is typically modeled by variations of the Lotka-Volterra competition equations (Volterra, 1926; Lotka, 1932). The position of a species in niche space is defined as the set of traits relevant to characterize resource utilization by this species. Proximity in such niche space, usually assumed to be onedimensional, implies utilization of similar resources which implies stronger competition. The question on whether populations in space can remain homogeneously distributed in the presence of competitive interactions or if rather they will break in clusters with a typical spacing is then related to important issues in population and community ecology such as the *principle of competitive exclusion* or the question on *limiting similarity* (MacArthur and Levins, 1967; May and MacArthur,

1972; Abrams, 1983; Barabás et al., 2012; Leimar et al., 2013).

The Lotka-Volterra equations or the related nonlocal FKPP model have been intensively analyzed in recent years (Fuentes et al., 2003; Scheffer and van Nes, 2006; Maruvka and Shnerb, 2006; Genieys et al., 2006; Pigolotti et al., 2007; Leimar et al., 2008; Hernández-García et al., 2009; Berestycki et al., 2009; Fort et al., 2009; Barabás et al., 2012; Leimar et al., 2013), from which a reasonable understanding of the dynamics they represent begins to emerge. At the same time, a different type of approach has been developed in which the competing organisms are modeled as individual agents following a stochastic dynamics (Hernández-García and López, 2004, 2005b; Birch and Young, 2006; Heinsalu et al., 2010, 2012, 2013). In this framework, the discrete nature of individual organisms and fluctuations associated to the birth-death processes are naturally taken into account. In addition, different types of spatial motion of the organisms can be implemented as different kinds of random walks. The dynamics of these *individual-based models* usually leads to results qualitatively and in some cases even quantitatively similar to the Lotka-Volterra approach. Some differences however arise related to the fluctuating and discrete nature of the particle system (Hernández-García and López, 2004; López and Hernández-García, 2004; Hernández-García and López, 2005a).

In this Paper we review some of the basic results on the dynamics of these stochastic and spatially extended discrete models of competing individuals. More general approaches to competition in spatial settings can be found for example in Klausmeier and Tilman (2002) or Amarasekare (2003). Our focus here is on the interplay between the competition interactions and the random motion of the individuals. Two types of random walks are considered: the standard Gaussian or Brownian random walk, and a family of Lévy flights characterized by a Lévy exponent  $\mu$  which controls the probability of large jumps (Metzler and Klafter, 2000; Klages et al., 2008; Méndez et al., 2014). The Lévy type of motion has been pointed out by its relevance in efficient search strategies (Benichou et al., 2011; James et al., 2011), and observed in a number of experimental studies (Dieterich et al., 2008; Matthäus et al., 2009, 2011; de Jager et al., 2011). We show that, under suitable conditions, competitive interactions lead to clustering and pattern formation. On the other hand, one of the main effects of the random motions of the individuals is to decrease and diffuse away inhomogeneities. Then the occurrence or not of population clusters will depend on the interplay between these two opposing forces. More surprisingly, another effect of the type of motion is to provide some competitive advantage to model organisms that are identical

in any other aspect: we will see that survival competition is mediated by clustering, so that forming stronger clusters, which depends on the random walk characteristics, provides better chances for survival.

Reviewing results on the above two effects of mobility on competition is the objective of this Paper. We try to put the different results into a common framework. First we present numerical simulations of the stochastic models, showing the main phenomenology and highlighting the basic mechanisms by means of heuristic arguments. Then we analyze suitable Lotka-Volterra integrodifferential models able to capture in a mean-field sense part of the observed phenomenology, pointing out also the limitations of such approach. For definiteness we concentrate in the situation of organisms competing for resources in physical space. Most of the results have also an interpretation in terms of species competition in niche space, but this will only be briefly commented in the Conclusions section.

In addition to summarizing previous results, and clarifying previously proposed heuristic arguments, we add here some new details on spatial structure of the competing populations and its relationship with competitive advantage, together with a study of extinction times of the different types of walkers. The Paper is organized as follows: in Sect. 2 we describe the stochastic model of interacting particles and in Sect. 3 we present the results of the numerical simulations, showing pattern formation, and their interpretation both in heuristic terms and with the help of a mean-field description. The limitations of this last approach are also pointed out. In Sect. 4 we put together walkers with different types of motion, competing between them, and focus on the phenomenon of competitive advantage by pattern formation. Quantitative details on spatial structure and extinction times are presented here, as well as a theoretical analysis in terms of a two-species mean-field description. Finally, in Sect. 5 we summarize and discuss our conclusions.

## 2. A model of competing bugs

We represent the state at time  $t$  of a set of simple competing organisms, reproducing asexually, by a set of  $N(t)$  point-like particles (they will also be referred as *walkers*, *bugs*, or *individuals*) at positions  $\mathbf{x}_i(t)$ ,  $i = 1, 2, \dots, N(t)$  in a twodimensional square domain of size  $L \times L$  (see López and Hernández-García (2004) for simulations of a onedimensional version). Periodic boundary conditions will be assumed, and without loss of generality we take  $L = 1$ .

The dynamics in the number of individuals includes birth and death processes which are affected by the competitive interactions. Namely, the bug labeled  $i$  reproduces and dies following Poisson processes of rates  $r_b^i$  and  $r_d^i$ , respectively, given by:

$$\begin{aligned} r_b^i &= \max(0, r_{b0} - \alpha N_R^i) \\ r_d^i &= r_{d0} + \beta N_R^i. \end{aligned} \tag{1}$$

$r_{b0}$  and  $r_{d0}$  are the constant reproduction and death rates experienced by an isolated bug. Competitive interactions are introduced in the terms containing  $\alpha$  and  $\beta$ : The reproduction rate of individual  $i$  decreases (we assume  $\alpha > 0$ ) with the number of neighbors,  $N_R^i$ , that are at a distance smaller than  $R$  ( $R < L$ ) from it. Analogously, death rate increases ( $\beta > 0$ ) with the number of neighbors. The newborns are placed at the same position as the parent bug, introducing reproductive correlations in the system. The max function in the first equation is needed to avoid rates (which are probabilities per unit of time) to become negative.

After each particle number update with the birth-death dynamics, the particles perform independent random walks. In the case of Brownian walks all particles make jumps in random directions and with sizes  $l$  independently sampled from the positive part of a Gaussian distribution of standard deviation  $\tilde{l} = (2\kappa\tau_0)^{1/2}$ . This defines a diffusion coefficient  $\kappa$ . It is convenient to perform the jumps after each particle-number updating, and  $\tau_0$  is the mean time between such events. The case of Lévy motion corresponds to the so-called Lévy flights (Klages et al., 2008; Metzler and Klafter, 2000): length  $l$  of the jumps is sampled from a Lévy-type probability density that for large  $l$  decays as  $\tilde{l}^{-1}(l/\tilde{l})^{-\mu-1}$ .  $\mu \in (0, 2)$  is the anomalous exponent controlling the probability of large jumps. The variance of the displacement is divergent, but an anomalous diffusion coefficient  $\kappa_\mu$  can be defined from  $\tilde{l}$ , the scale parameter:  $\tilde{l} = (2\kappa_\mu\tau_0)^{1/\mu}$ . When particles move freely without undergoing the birth-death process, their spatial distribution develops fat tails at long distances, which is an anomalous-diffusion behavior very different from the Gaussian one (Klages et al., 2008; Metzler and Klafter, 2000). The smaller  $\mu$  the more anomalous the diffusion process. When  $\mu > 2$ , however, the variance of the displacements becomes finite and the central limit theorem guarantees that Gaussian statistics applies at long times. We will see that the effect of the anomalous diffusion is not so drastic in the presence of the birth-death process or the finite interaction range  $R$ , since these quantities

provide effective time and space cut-offs before the asymptotic behavior is attained. Both  $\kappa$  and  $\kappa_\mu$  will be denoted loosely as *diffusivities*. The dynamics defined in this way incorporates interactions in the birth-death dynamics, whereas the random walks of the individuals remain independent (except at the moment of birth which fixes initial position). We are thus exploring mechanisms which are different, and complementary, from the ones labeled as *active Brownian particles* (Romanczuk et al., 2012), in which interactions affect motion and not the particle number.

The processes specified above are implemented here through the Gillespie algorithm as described in Heinsalu et al. (2012), where additional details on the numerics can be found. Other implementations are possible, which lead to similar results. For example Hernández-García and López (2004) used a discrete-time approach nearly equivalent to the present one, except for very large Poisson rates which become limited by the minimum time imposed in the time discretization.

Parameter  $R$  is a central ingredient in our model, as it imposes a finite range for the competitive interactions. In fact we will see that the periodicity of the spatial patterns that are described below is directly related to  $R$ . In this paper we will focus in the situation in which  $R$  is much smaller than system size  $L$  (typically we take  $R = 0.1$  as compared to  $L = 1$ ) so that boundary conditions become relatively irrelevant. On the other hand, periodic-pattern formation requires  $R$  to be substantially larger than the sizes of particle clusters (see Sect. 3.1). This will be achieved by considering small values of the diffusivities introduced above.

### 3. Clustering of particles and pattern formation

#### 3.1. The competitive clustering instability

In simulations of Brownian or Lévy bugs with a sufficiently large  $\kappa$  or  $\kappa_\mu$ , respectively, a nearly homogeneous distribution of particles is attained which remains fluctuating but statistically steady. The expected density in such situation can be estimated from the requirement of a balance between births and deaths. From Eq. (1) and neglecting the max condition (which is correct if we neglect fluctuations) this is achieved when  $N_R^i \approx (r_{b0} - r_{d0})/(\alpha + \beta)$ . In a homogeneous situation the expected density  $\rho_0$  is the same everywhere, and since  $N_R^i$  counts the number of particles in a circle of area  $\pi R^2$ , we have

$$\rho_0 = \frac{\Delta}{\gamma \pi R^2} \quad (2)$$

where the notation

$$\Delta \equiv r_{b0} - r_{d0} \quad \text{and} \quad \gamma \equiv \alpha + \beta \quad (3)$$

has been introduced. This estimation is correct for sufficiently large  $\Delta$ . For small  $\Delta$  the expected density is small and stochastic extinctions are likely to occur from fluctuations in the particle number. In this case, in average, the expected density becomes smaller than (2) and even vanishes well above  $\Delta = 0$  (Hernández-García and López, 2004; López and Hernández-García, 2004; Hernández-García and López, 2005a).

But the most interesting dynamics occur when diffusivities are sufficiently small. In this situation the homogeneous density breaks down and an approximately periodic arrangement of particle clusters arise, both for Brownian as for Lévy walkers (see Fig. 1). The symmetry of the resulting pattern is roughly hexagonal. Configurations such as the ones in Fig. 1 can be analyzed with different types of correlations and structure functions (Hernández-García and López, 2004; López and Hernández-García, 2004; Birch and Young, 2006; Ramos et al., 2008; Heinsalu et al., 2010). We delay this type of analysis until section 4, where it will be used to characterize competition between different types of walkers. In the following we just comment on the main aspects: Most of the parameters used in the three simulations illustrated in Fig. 1 are equal, the only differences being the use of Brownian (panels (a) and (c)) or Lévy (panel (b)) jumps, and the presence of competition only in the birth rate (panels (a) and (b)) or only in the death rate (panel (c)). In the three cases the number of particles is similar (fluctuating close to 2600) as well as the number of well-formed clusters (63, 68 and 62 for panels (a), (b) and (c), respectively). The main difference is in the shape of the clusters and in their ordering: In the Lévy case, because of the larger probability of long jumps, there are much more *solitary* particles (Heinsalu et al., 2010, 2012) that jump into the regions between clusters, remaining there for a short time before dying or jumping again. In the Gaussian case clusters are much more compact. When competition affects only the death rate (panel (c)) clusters are narrower and are arranged in a more disordered way. The reasons for this will be commented at the end of subsection 3.3.

One can understand the instability of the homogeneous distribution by some qualitative arguments that clearly indicate that it is a consequence of the competitive interactions: Let us consider the bugs initially distributed homogeneously in space with the density  $\rho_0$ , so that deaths and births are

balanced. When there are fluctuations or perturbations that enhance the density at points separated by a distance larger than  $R$  but smaller than  $2R$ , death will become more probable than reproduction in the area in between these density maxima. This is so (see Fig. 2) because of Eqs. (1) and of the fact that in this zone an individual experiences the competition with the organisms from at least two of the density maxima, whereas in each density maximum the competition takes place only between the individuals in the same maximum (other maxima are simply out of the interaction range  $R$ ). As a consequence, the density will decrease in between the density maxima. This in turn releases competitive pressure on the maxima, which will tend to grow, and then start to form periodically located clusters (at a distance  $fR$ , with  $1 < f < 2$ ) and close a positive feedback loop that will finally eliminate all organisms in these *death zones* between the clusters. The only mechanism that can stop this process is particle diffusion, if it occurs fast enough to redistribute the bugs before the instability concentrates them.

The above qualitative argument clearly identifies the competitive interactions as responsible for the pattern forming instability. However it requires, besides small diffusivities to guarantee that clusters do not extend into the *death zones*, that there is a sufficiently sharp distinction between the interior and the exterior of the competition area. The precise meaning of these requirements will be clarified in the next subsection. We close this one by noticing that the number of particles in the system in which clustering occurs is higher than what would be allowed by the homogeneous distribution. To see this we recall the previous calculation of  $\rho_0$  in which  $N_R^i$  bugs are distributed in an area  $\pi R^2$ . Now (Fig. 1) the same number of bugs is concentrated in small clusters in the center of regions which are approximately hexagons of apothem  $fR/2$ . Since the area of such hexagons is much smaller than the area of the circle of radius  $R$  (this is so as far as  $f < 2.199$ ) the mean density is higher and we have more particles in the system. The hexagonal shape is not necessary for the argument; it is enough that clusters are associated to regions of width  $fR$ , with  $f < 2$ , instead of circles of diameter  $2R$ . By clustering together and leaving in between sufficient space free from competitors (i.e. leaving empty the death zones), the bugs experience a smaller effective competition and can survive in larger numbers.

### 3.2. Mean-field approach

Let us analyze a deterministic description of the system, which is enough to formalize the heuristic arguments given above. Denoting the mean local



density of walkers by  $\rho(\mathbf{x}, t)$ , different mathematical arguments (Hernández-García and López, 2004; Birch and Young, 2006) can be put forward to justify that, if statistical fluctuations are neglected, the following dynamics approximates the mean evolution of the density:

$$\frac{\partial \rho(\mathbf{x}, t)}{\partial t} = M(\mathbf{x}, t)\rho(\mathbf{x}, t) + D\rho(\mathbf{x}, t). \quad (4)$$

Here,  $D$  stands for the diffusion-like operator representing the effect of mobility on the particle density. For Brownian walkers, it is the simple diffusion operator  $D = \kappa \nabla^2$ , whereas in the Lévy case  $D = \kappa_\mu \nabla^\mu$  involves the fractional derivative of order  $\mu$  (Metzler and Klafter, 2000; Klages et al., 2008; Méndez et al., 2014). The quantity  $M(\mathbf{x}, t)$  is

$$M(\mathbf{x}, t) \equiv \Delta - G_{\mathbf{x}} * \rho, \quad (5)$$

which simply the difference between birth and death rates from Eq. (1).  $\Delta$ , defined in (3), is a net linear growth rate. The symbol  $G_{\mathbf{x}}*$  denotes the convolution product with a kernel  $G(\mathbf{x})$ , i.e.,

$$G_{\mathbf{x}} * f \equiv \int d\mathbf{y} G(\mathbf{x} - \mathbf{y})f(\mathbf{y}), \quad (6)$$

where the integration is over all the system domain. In our case, in which interactions enter the dynamics via Eq. (1) which counts the number of organisms in a two-dimensional neighborhood of radius  $R$ , the kernel  $G(\mathbf{x})$  is:

$$G(\mathbf{x}) = \begin{cases} \gamma, & \text{if } |\mathbf{x}| < R, \\ 0, & \text{elsewhere,} \end{cases} \quad (7)$$

being  $\gamma$  the competition slope defined in (3). The above notation is general enough to be useful in cases of arbitrary dimensionality and when the interaction differs from (7), for example if it is weighted with the distance (Birch and Young, 2006; Pigolotti et al., 2007; Hernández-García et al., 2009; Pigolotti et al., 2010).

The type of description given by Eq. (4) turns out to be accurate where the densities are large enough to neglect fluctuations. We also mention that the use of the operators  $\nabla^2$  and  $\nabla^\mu$  defining  $D$  is accurate only at sufficiently large time and spatial scales. Numerical simulation of Eq. (4) for low diffusivities correctly exhibits the pattern forming instability leading to an hexagonal

pattern with a periodicity similar to the one observed in the particle simulations (Hernández-García and López, 2004; López and Hernández-García, 2004; López and Hernández-García, 2007a).

We now use this continuous description to understand analytically the pattern forming instability. To do so, we introduce some notation: we call  $\hat{G}_{\mathbf{k}}$  the Fourier transform of  $G(\mathbf{x})$ , i.e.,  $\hat{G}_{\mathbf{k}} = \int d\mathbf{x} e^{i\mathbf{k}\cdot\mathbf{x}} G(\mathbf{x})$ , and  $\hat{G}_0 \equiv \hat{G}_{\mathbf{k}=\mathbf{0}} = \int d\mathbf{x} G(\mathbf{x})$ . For our two-dimensional kernel (7) these functions become:

$$\begin{aligned}\hat{G}_{\mathbf{k}} &= 2\gamma\pi R^2 \frac{J_1(kR)}{kR} \\ \hat{G}_0 &= \gamma\pi R^2 ,\end{aligned}\tag{8}$$

with  $J_1$  being the first-order Bessel function and  $k = |\mathbf{k}|$ . Also, the action of the operator  $D$  in the Fourier representation involves simple multiplications:  $\hat{D}(k) = -\kappa k^2$  in the Brownian case or  $\hat{D}(k) = -\kappa_\mu k^\mu$  under Lévy motions.

The spatially homogeneous steady solution of Eq. (4) is precisely  $\rho_0$  in (2), which is independent of the particular form of the operator  $D$ . Now we perturb  $\rho_0$  with harmonic functions and look at the growth rates of such perturbations to assess stability:

$$\rho(\mathbf{x}, t) = \rho_0 + \epsilon e^{\lambda(\mathbf{k})t} e^{i\mathbf{k}\cdot\mathbf{x}}.\tag{9}$$

Linearizing in the small perturbations  $\epsilon$  one finds

$$\lambda(\mathbf{k}) = \hat{D}(k) - \Delta \frac{\hat{G}_{\mathbf{k}}}{\hat{G}_0}.\tag{10}$$

Since  $\hat{D}(k) < 0$ , we see that  $\lambda(\mathbf{k})$  will remain negative, and then  $\rho_0$  will remain stable, when  $\hat{G}_{\mathbf{k}}$  is positive  $\forall \mathbf{k}$ . When  $\hat{G}_{\mathbf{k}}$  is negative for some  $\mathbf{k}$ , however, the second term can destabilize the homogeneous solution if the mobility term characterized by  $\hat{D}(k)$  is not sufficiently negative at these wavenumbers. The change from negative to positive sign in  $\lambda(\mathbf{k})$  will occur first for the wavenumber  $k_c = |\mathbf{k}_c|$  for which  $\lambda(\mathbf{k})$  is maximum. The instability will develop in a periodic pattern which, at least close enough to the instability (Cross and Hohenberg, 1993), will have a periodicity  $\delta$  determined by the growing wavenumber,  $\delta = 2\pi/k_c$ . Equation (10) clearly expresses the first effect of particle mobility characterized by  $\hat{D}(k)$  on the competitive dynamics:  $\hat{D}(k_c) < 0$  will stabilize the instability produced by the negative values of  $\Delta\hat{G}_{\mathbf{k}}/\hat{G}_0$  at  $|\mathbf{k}| \approx k_c$  until they are too large. From the expressions  $\hat{D}(k_c) = -\kappa k_c^2$  or  $-\kappa_\mu k_c^\mu$  we can identify these quantities as the rates

of particle-escape out of the periodic structures of wavenumber  $k_c$ : increased diffusivities enhance the flux of particles from the clusters towards the death zones, thus working against the pattern formation process (and reducing the mean density).

The qualitative requirement discussed in subsection 3.1 of a *sufficiently sharp distinction between the interior and the exterior of the competition area* becomes now formalized: the sharp distinction occurs when the Fourier transform  $\hat{G}_{\mathbf{k}}$  of the kernel takes negative values. For example, for kernels of the form  $G(\mathbf{x}) \propto \exp(-|\mathbf{x}/\sigma|^p)$ , the Fourier transform has negative components (Bochner, 1937), and then they are sufficiently sharp to produce the competitive instability, in the platykurtic situation  $p > 2$  (note that the flat-top kernel in (7) corresponds to  $p \rightarrow \infty$ ). Under kernels with  $p \leq 2$  (which include the Gaussian and the exponential kernels)  $\hat{G}_{\mathbf{k}}$  is positive and then the homogeneous distribution will remain stable.

We now return to the specific competition kernel given by (7) and (8). We introduce dimensionless versions of the wavenumber,  $q \equiv kR$ , and of the growth rate,  $\Lambda(q) \equiv R^\mu \lambda(\mathbf{k})/\kappa_\mu$  for the Lévy case. The corresponding expressions in the Gaussian case are obtained by using  $\mu = 2$  and replacing  $\kappa_2$  by  $\kappa$ . Equation (10) then reads

$$\Lambda(q) = -q^\mu - \nu \frac{J_1(q)}{q}, \quad (11)$$

where the dimensionless combination  $\nu \equiv 2R^\mu \Delta/\kappa_\mu$  has been introduced. We plot Eq. (11) in Fig. 3 for the Gaussian case (formally obtained by substituting  $\mu = 2$ ) and for a Lévy case with  $\mu = 1$ . We have that pattern formation occurs when  $\nu > \nu_c$ , which can be achieved by increasing  $R$  or  $\Delta$ , or reducing the diffusivity  $\kappa_\mu$ .

The critical wavenumber  $k_c = q_c/R$  for which instability first occurs can be found by solving simultaneously the equations  $\Lambda(q_c) = 0$  and  $\Lambda'(q_c) = 0$ , which implement the conditions of change of sign in the growth rate and of maximum of the growth rate, respectively. Using these conditions and properties of derivatives of Bessel functions one obtains the critical value of  $\nu$ :  $\nu_c = -q_c^{\mu+1}/J_1(q_c)$  and the equation for the critical wavenumber:

$$q_c \frac{J_2(q_c)}{J_1(q_c)} = -\mu. \quad (12)$$

Numerical solution of this equation gives  $q_c = q_c(\mu)$  ( $= k_c R$ ) from which the expected periodicity of the pattern is  $\delta = 2\pi R/q_c$ . Table 1 presents these

quantities for several values of  $\mu$  and for the Gaussian case. In agreement with the previous heuristic discussion, we see that pattern periodicity (last column in the Table) is always of the form  $\delta = fR$ , with  $1 < f < 2$ .

### 3.3. Limitations of the deterministic description

The predicted periodicity is in good agreement with numerical simulations (Hernández-García and López, 2004; Heinsalu et al., 2010), which confirms the relevance of the nonlocal KPP equation (4) to describe the particle system. There is only a weak dependence of the wavenumber on diffusivities which is not predicted by the mean-field approach. But there are other features that are not captured by this deterministic description:

First, as already commented, the homogeneous solution  $\rho_0$  in (2) overestimates the mean density when  $\Delta$  is small. Because of number fluctuations, the particle system becomes extinct when  $\Delta$  is still positive. This transition is of the Directed Percolation type (López et al., 2007b), qualitatively different from the mean-field transition to the extinct state predicted by Eq. (4) at  $\Delta = 0$ , but that can be recovered by incorporating multiplicative noise terms to it (Ramos et al., 2008).

Second, even if pattern periodicity is correctly described by (4), cluster width is not. Extreme discrepancy occurs when  $R$  grows to be of the order of the system size, in which case solutions of (4) give a patch occupying the whole system, whereas the particles in the discrete model remain aggregated in a single small cluster (Hernández-García and López, 2005b; Heinsalu et al., 2012). In fact cluster width, as in Young et al. (2001), is determined by reproductive correlations: it is essentially (Hernández-García and López, 2005a; Heinsalu et al., 2012) the distance  $(2\kappa\tau_d)^{1/2}$  or  $(2\kappa_\mu\tau_d)^{1/\mu}$  traveled during a particle lifetime  $\tau_d \approx (r_d^i)^{-1}$  (see Hernández-García and López (2005b) for a refinement that takes into account the lifetime of the *lineage* of a particle). Olla (2012) discusses how different mobility types affect reproductive correlations in noninteracting particle systems.

As a third deficiency of the deterministic modeling we point out that, although for the parameter values used in panels (a) and (c) of Fig. 1 the corresponding instances of Eq. (4) are identical, particle configurations are indeed quite different. As noted before, the spacing between clusters is very similar, but clusters in (c) are narrower and are arranged in a more irregular way. Both differences have the same origin: In Eq. (4) only the difference between the birth and death rates enter. But for the stochastic model the absolute value of the rates is also relevant. For example, if we balance the

birth and death rates (neglecting the diffusivities) to obtain steady values  $r_b^{st}$  and  $r_d^{st}$ , we find  $r_b^{st} = r_d^{st} = r_{d0} + \beta\Delta/(\alpha + \beta)$ , which is an increasing function of  $\beta$ . Thus, giving increasing weight to competition in the death term while keeping other parameters such as  $\Delta$  or  $\gamma$  unchanged increases the value of the rates in steady state. The smaller width of the clusters in panel (c) of Fig. 1 with respect to the ones in panel (a) is a consequence of the smaller lifetime of the bugs because of the increased steady death rate. Also, the rate parameter in a Poisson process not only fixes the mean number of events per unit of time, but also its variance. Then higher rates produce more fluctuating processes (Heinsalu et al., 2012), even if the mean value of the difference between birth and death rates remains constant. This explains the larger irregularity of the pattern in panel (c) of Fig. 1 with respect to panel (a) which has  $\beta = 0$  and then smaller steady value of the rates. This effect, as others linked to fluctuations, is absent from Eq. (4). Another possible consequence of fluctuations that we have not studied in detail could be the appearance of quasipatterns excited by noise (Butler and Goldenfeld, 2011) even in parameter regions in which the deterministic description predicts a homogeneous state.

## 4. Clustering as a competitive advantage

### 4.1. Two-species competition

In Sect. 3 we have seen how competitive interactions with some features lead to particle clustering and pattern formation, and how particle mobility works against this and shapes the pattern characteristics. In this section we present a different phenomenon: competition advantage provided by clustering. We consider competition between two types of bugs (we can think of them as pertaining to two species), identical in every aspect except in the type of motion. We will see that despite having the same birth and death rates, and identical direct competition properties, the different clustering characteristics associated to the different type of random walk provide a competitive advantage to one of the species (roughly the one forming the narrowest clusters). When competing together one of the species survives and the other gets extinct.

The model set-up is as before, except that initially half of the individuals are Brownian random walkers characterized by the diffusion coefficient  $\kappa$  and the other half are Lévy random walkers characterized by the exponent  $\mu$  and the anomalous diffusion coefficient  $\kappa_\mu$ . Birth and death rates are the same

as before for the two species, Eq. (1), with  $N_R^i$  counting all neighbors (i.e., of any type) of bug  $i$ . When reproducing, offspring is of the same type as the parent walker.

When  $\kappa$  and  $\kappa_\mu$  are sufficiently large (Heinsalu et al., 2013), walkers appear to be distributed in an unstructured way, as when a single species is present. Local fluctuations occur around an homogeneous mean without a long-lasting pattern forming. The population numbers of the two types of walkers widely fluctuate in antiphase, whereas the total number weakly fluctuates close to a well-defined value. In this situation in which both species are highly diffusive, the two types of walkers become well mixed, so that there is no difference in the neighborhood seen by the individuals of one or the other type. Thus, effectively, the two species become equivalent. The observed neutral fluctuations that conserve the total number were expected from the stochasticity of the reproduction-death process and the equivalence between the species. After some time, however, neutral fluctuations can create diffuse patches dominated by a single species, and eventually a particular neutral fluctuation could eliminate all individuals of a given type, after which only the other species will remain in the system. The winner is not a better competitor, it is just determined by chance.

The situation becomes different when  $\kappa$  or  $\kappa_\mu$  decrease (Heinsalu et al., 2013). When one of these quantities becomes sufficiently small the corresponding species begins to form clusters, in a manner similar to the one discussed in Sect. 3. At this moment the population of the other species begins to decrease until complete extinction. The possibility to develop clusters, determined by the type of motion, has given a competitive advantage to one of the species. When the simulation is started with the two types of bugs randomly mixed and the values of  $\kappa$  and  $\kappa_\mu$  are such that both species form periodic patterns when alone, then clusters begin to form and the bugs compete, until typically only one of the species survives. The observed outcome at some particular values of the birth/death parameters is summarized in Fig. 4. Variables in the axes are  $|\hat{D}_\mu(k_L)| = \kappa_\mu k_L^\mu$  (with  $\mu = 1$ ) and  $|\hat{D}_2(k_B)| = \kappa k_B^2$ .  $k_B$  is the critical wavenumber  $k_c$  for which instability first occur in the Brownian walker case, whereas  $k_L$  is the critical  $k_c$  in the Lévy case. Both quantities can be read-off from Table 1. This scaling of the axes is suggested by the analytical approach of subsection 4.4. For now it is enough to keep in mind that these quantities are proportional to the diffusivities  $\kappa_\mu$  (with  $\mu = 1$ ) and  $\kappa$ . We see that when one of the diffusivities is sufficiently

small, the corresponding species wins. There is also a small region in which coexistence persists during all the long simulation times. At variance with the case of large diffusivities, here the coexisting species are not mixed but occupy segregated clusters, and both particle numbers, not just their sum, fluctuate around well-defined means. There are also some transition regions where the outcome depends on the initial condition or the particular random realization. When approaching these transitions zones, the extinction times of the loosing species grow and finally diverge, signaling a change of winner. This will be quantified in subsection 4.3.

By comparing visually the type of patterns formed by each of the two species when they are alone in the system one recognizes that, roughly, the organisms forming more concentrated and populated clusters (which is associated to lower diffusivities) are more successful when put into competition with the other species. We quantify this observation in subsection 4.2 by comparing spatial patterns in terms of radial distribution functions. Before that we mention that the general trends of winner and loosing species can be understood from the heuristic arguments set up in Sect. 3.1: the existence of *death zones* in between particle groups would develop the same clustering instability as before for both species, but this is opposed by the flux of particles out of the clusters because of their random walks. The species for which this flux is higher, which manifest in wider clusters or in its absence, will visit more frequently the *death zones* and this gives them a clear competitive disadvantage with respect to the ones that remain in well concentrated clusters. The next subsection will quantify this relationship between cluster compactness and competition outcome and, after subsection 4.3 devoted to extinction times, we will formalize these intuitive ideas in 4.4 to provide some quantitative criterion about competition outcome.

#### 4.2. *Spatial structures in single-species simulations*

To understand the conditions favoring the surviving of one or the other species, we return in this subsection to the situation in which only one species is present in the system and investigate their radial distribution function  $g(r)$ . It is defined by using the formula  $dn = (N/L^2)g(r)2\pi r dr$  which involves the number of particles  $dn$  at a distance between  $r$  and  $r + dr$  from a specific one, and then averaging over all these specific particles and over long times.  $N$  is the total number of particles in the simulation domain of area  $L^2$ .  $g(r)$  describes (Dieckmann et al., 2001) how the density varies with the distance

from a given particle with respect to the uniform distribution (characterized by  $g(r) = 1$ ).

The value of  $g(r \rightarrow 0)$  gives an idea of the number of close neighbors surrounding any individual, i.e., it indicates the increase in local density, induced by the presence of one of the organisms, with respect to the uniform density. The presence of the first peak of  $g(r)$  at  $r \neq 0$  indicates the formation of a periodic pattern with periodicity  $r$ . The value of  $g(r)$  in between the first two peaks measures the density between clusters compared to the uniform distribution. The higher and narrower the peak at  $r \rightarrow 0$ , the more concentrated are the organisms in the clusters.

In Fig. 5 we depict  $g(r)$  for the two types of walkers and for different values of  $\kappa$  and  $\kappa_\mu$ . The three chosen values of  $\kappa_\mu$  are intended to represent the three qualitatively different situations seen in Fig. 4 for the case of competing walkers: for  $\kappa_\mu = 4 \times 10^{-4}$ , which corresponds in the figure to  $|\hat{D}_\mu(k_L)| = 0.0198$ , Lévy walkers always win; for  $\kappa_\mu = 4 \times 10^{-2}$  ( $|\hat{D}_\mu(k_L)| = 1.98$ ) Brownian walkers win; for  $\kappa_\mu = 4 \times 10^{-3}$  ( $|\hat{D}_\mu(k_L)| = 0.198$ ), depending on the value of  $\kappa$ , there is either coexistence of the two species or Lévy or Brownian walkers win the competition.

The value of  $g(r \rightarrow 0)$  for the Lévy walkers with the smallest value of  $\kappa_\mu$  or  $|\hat{D}_\mu(k_L)|$  plotted in Fig. 5 is higher than for Brownian walkers with any of the values of  $\kappa$  considered. This means that Lévy clusters are relatively more populated than Brownian ones in this range of parameters (see also Heinsalu et al. (2010, 2012)). Instead, for the largest value of  $\kappa_\mu$  or  $|\hat{D}_\mu(k_L)|$  there is no clustering of Lévy walkers ( $g(r) \approx 1$ ) and the value of  $g(r \rightarrow 0)$  is always larger for the systems of Brownian walkers with the studied values of  $\kappa$ . In the first case the Lévy walkers win, whereas in the second case the Brownian walkers win, suggesting that in the two-species model the survival is favored by the stronger clustering.

The situation is a bit more complex for the intermediate value  $\kappa_\mu = 4 \times 10^{-3}$  ( $|\hat{D}_\mu(k_L)| = 0.198$ ). As can be seen from the radial distribution function (Fig. 5), Lévy walkers do not form a clear periodic structure, although there is still weak local clustering as indicated by  $g(r \rightarrow 0) > 1$ . But clustering is even weaker for the Brownian walkers with  $\kappa = 10^{-4}$  ( $|\hat{D}_2(k_B)| = 0.23$ ). Because the value of  $g(r \rightarrow 0)$  is sufficiently higher in the system of Lévy walkers, the latter ones win the competition. When reducing the Gaussian diffusivity to  $\kappa = 6 \times 10^{-5}$  ( $|\hat{D}_2(k_B)| = 0.137$ ) the difference of  $g(r \rightarrow 0)$  between the Lévy and Brownian systems is rather small and the winner of the competition is



a random event. Reducing further  $\kappa$  to  $\kappa = 4 \times 10^{-5}$  ( $|\hat{D}_2(k_B)| = 0.091$ ) the values of  $g(r \rightarrow 0)$  are approximately equal in the Lévy and Brownian systems; in this case, however, a clearer cluster periodicity in the Brownian case (larger value of the the first peak of  $g(r)$  at  $r \neq 0$ ) seems to give them advantage over the Lévy ones.

Following this observation that competition success is attained by the motion leading to the strongest and clearest clustering, one would guess that reducing further  $\kappa$  to  $\kappa = 4 \times 10^{-6}$  ( $|\hat{D}_2(k_B)| = 0.0091$ ) with the Lévy diffusivity still at  $\kappa_\mu = 4 \times 10^{-3}$  the Brownian walkers would win. However, as indicated by Fig. 4, this is not the case. Instead, coexistence occurs. This situation will be commented at the end of next subsection.

### 4.3. Extinction times

We return to the situation in which both species are initially present in the system and investigate now the average time  $\tau$  that it takes for one of the two competing species to go extinct (known as fixation time in the population genetics jargon). Notice that, since we study a finite system, all species will become extinct due to large fluctuations at sufficiently long times. However, in the case of systems consisting of at least some hundreds of individuals this happens only after very long time scales. In our simulations we have never observed such complete extinction and we report only the fixation time for the species dying out first. Figure 6 displays the fixation time,  $\tau$ , as a function of the diffusion coefficient,  $\kappa$ , of the Brownian walkers for different values of the anomalous diffusion coefficient,  $\kappa_\mu$ , of the Lévy walkers.

For  $\kappa_\mu = 4 \times 10^{-4}$ , when the Lévy walkers always win ( $|\hat{D}_\mu(k_L)| = 0.0198$ , see Fig. 4), the fixation time,  $\tau$ , decreases when increasing  $\kappa$ , i.e., the Brownian walkers die out faster for larger diffusion coefficient. Namely, larger  $\kappa$  means weaker clustering of the Brownian bugs, thus confirming the observation made in subsection 4.2 of decreased stability for weaker clustering.

In the largest value  $\kappa_\mu = 4 \times 10^{-2}$ , which corresponds to the situation when Brownian walkers win ( $|\hat{D}_\mu(k_L)| = 1.98$ , see Fig. 4), the fixation time,  $\tau$ , increases for larger values of  $\kappa$ . The stronger clustering of Brownian walkers leads to the extinction of Lévy ones which form essentially no clusters. The extinction of the Lévy walkers is delayed by weaker clustering of Brownian walkers, i.e., by larger  $\kappa$ , which makes the two species more similar.

For the intermediate value  $\kappa_\mu = 4 \times 10^{-3}$  ( $|\hat{D}_\mu(k_L)| = 0.198$ ), when the outcome of the competition depends on the value of  $\kappa$ , the general behavior of  $\tau(\kappa)$  is the same as for  $\kappa_\mu = 4 \times 10^{-4}$ , i.e., for larger values of  $\kappa$  the

extinction time is smaller, increasing rapidly when decreasing  $\kappa$ . The local maximum in  $\tau(\kappa)$  is associated with the transition from the regime where Lévy walkers win due to their stronger clustering to the regime where the Brownian walkers win due to their stronger clustering; for this point it is a random event which of the two species, characterized by a similar capability of clustering, wins the competition.

As noted at the end of subsection 4.2, for the intermediate values of  $\kappa_\mu$  (e.g., for  $\kappa_\mu = 4 \times 10^{-3}$ ) such that the Lévy walkers still form clusters but not too strong ones, and diffusion coefficient  $\kappa$  of the Brownian walkers becomes very small, the Lévy walkers do not die out but coexistence of the two species occurs, i.e., during the accessible simulation time we do not observe the extinction of neither of the competing species ( $\tau \rightarrow \infty$  for  $\kappa \rightarrow 0$ ). In this situation, what happens is that the Brownian walkers form very strong clusters that the Lévy walkers are not capable to invade (because its larger flux out brings them to the death zones). At the same time, due to the extremely low diffusion and the high death rate in the inter-clusters space, the Brownian walkers are not capable to travel away and colonize the territories that have been occupied by the Lévy walkers during the initial cluster formation period due to the fluctuations.

#### 4.4. Two-species mean-field description

We now analyze a mean-field deterministic description of the system, in order to understand the relative stability of Lévy *versus* Brownian bugs under competition. Denoting the local density of Brownian walkers by  $\rho_B(\mathbf{x}, t)$  and by  $\rho_L(\mathbf{x}, t)$  the corresponding to the Lévy ones, the dynamics (4) becomes now:

$$\begin{aligned} \frac{\partial \rho_B(\mathbf{x}, t)}{\partial t} &= M(\mathbf{x}, t)\rho_B(\mathbf{x}, t) + D_2\rho_B(\mathbf{x}, t), \\ \frac{\partial \rho_L(\mathbf{x}, t)}{\partial t} &= M(\mathbf{x}, t)\rho_L(\mathbf{x}, t) + D_\mu\rho_L(\mathbf{x}, t), \end{aligned} \tag{13}$$

where the difference between birth and death rates is now  $M(\mathbf{x}, t) \equiv \Delta - G_{\mathbf{x}*}(\rho_B + \rho_L)$ . The notation  $D_2$  has been introduced to specify the Brownian diffusion operator  $D_2 \equiv \kappa\nabla^2$  and analogously  $D_\mu \equiv \kappa_\mu\nabla^\mu$ .

Interaction of the two competing species via Eq. (13) is clearly a fully non-linear problem that can not be addressed analytically in a complete manner. But we will see that a linear analysis around the homogeneous states gives some insight into the process. We first look for the spatially homogeneous solutions of Eqs. (13). In this case the spatial derivatives vanish and there is

no difference between the dynamics of the two species. There exists a family of steady homogeneous solutions satisfying the condition  $\rho_B + \rho_L = \Delta/\hat{G}_0$ . Thus, we can write the members of such a family in terms of a parameter  $a \in [-\Delta/(2\hat{G}_0), \Delta/(2\hat{G}_0)]$ :

$$\rho_B^0 = \frac{\Delta}{2\hat{G}_0} + a, \quad \rho_L^0 = \frac{\Delta}{2\hat{G}_0} - a. \quad (14)$$

The upper boundary of this family ( $a = \Delta/(2\hat{G}_0)$ ) corresponds to the pure Brownian population, whereas the lower boundary ( $a = -\Delta/(2\hat{G}_0)$ ) corresponds to the pure Lévy population. Intermediate values of  $a$  parameterize different degrees of homogeneous coexistence.

To demonstrate that all this homogeneous family is stable for sufficiently high values of the diffusivities  $\kappa$  and  $\kappa_\mu$  we perturb it with harmonic functions and calculate the growth rates of such perturbations:

$$\begin{aligned} \rho_B(\mathbf{x}, t) &= \rho_B^0 + \delta_B e^{\lambda t} e^{i\mathbf{k}\cdot\mathbf{x}}, \\ \rho_L(\mathbf{x}, t) &= \rho_L^0 + \delta_L e^{\lambda t} e^{i\mathbf{k}\cdot\mathbf{x}}. \end{aligned}$$

Linearizing with respect to the small perturbations  $\delta_B$  and  $\delta_L$ , one gets a linear system for which the solvability conditions give a quadratic equation for  $\lambda$ , with two solutions for each value of the set of parameters and of  $k$ :

$$\lambda_{\pm} = -\frac{1}{2}A \pm \frac{1}{2}\sqrt{A^2 - 4(BC - D)}, \quad (15)$$

with

$$A = \Delta \frac{\hat{G}_{\mathbf{k}}}{\hat{G}_0} + |\hat{D}_2(k)| + |\hat{D}_\mu(k)|, \quad (16)$$

$$B = \hat{G}_{\mathbf{k}} \left( \frac{\Delta}{2\hat{G}_0} + a \right) + |\hat{D}_2(k)|, \quad (17)$$

$$C = \hat{G}_{\mathbf{k}} \left( \frac{\Delta}{2\hat{G}_0} - a \right) + |\hat{D}_\mu(k)|, \quad (18)$$

$$D = \hat{G}_{\mathbf{k}}^2 \left[ \left( \frac{\Delta}{2\hat{G}_0} \right)^2 - a^2 \right]. \quad (19)$$

We use the absolute value for  $|\hat{D}_2(k)| = -\hat{D}_2(k) = \kappa k^2$  and  $|\hat{D}_\mu(k)| = -\hat{D}_\mu(k) = \kappa_\mu k^\mu$  to stress that these quantities are positive. For sufficiently

large diffusivities  $\kappa$  and  $\kappa_\mu$ ,  $|\hat{D}_2(k)|$  and  $|\hat{D}_\mu(k)|$  are large and the values of  $\lambda_+$  and  $\lambda_-$  are negative (except for the zero mode  $\lambda_+(k=0) = 0$ ), meaning that any perturbation applied to a member of the family of homogeneous solutions decays (except the neutral perturbations associated to the zero mode, which transform one of the homogeneous solutions into another one), and thus any of the homogeneous solutions is stable. No persistent pattern can appear in the system for large values of  $\kappa$  and  $\kappa_\mu$ . At each instant the system is in one of the homogeneous states described by Eqs. (14). In the presence of noise caused by the random birth-death process (absent from Eqs. (13)) continuous fluctuations in the direction of the neutral mode (equivalent to fluctuations in  $a$ ), will occur transforming one of the homogeneous states into another one.

When decreasing  $\kappa$  or  $\kappa_\mu$  ( $\hat{D}_2(k)$  or  $\hat{D}_\mu(k)$  approaching zero) the largest of the growth rates in Eq. (15) becomes positive at some values of  $k$ . This identifies a pattern-forming instability leading to periodic modulations of the densities with a characteristic periodicity given by  $2\pi/k$ , similarly to the cases of a single species described in Sect. 3. Some information on the character of the instability evolution can be gained by focussing in its linear growth phase. In particular one can ask what is the homogeneous combination of Lévy and Brownian bugs that becomes unstable first when decreasing the values of  $\kappa$  and  $\kappa_\mu$ . The instability condition occurring first is  $\lambda_+ > 0$ , which from Eq. (15) implies  $BC < D$ . By using Eqs. (16)-(19), this happens if

$$|\hat{D}_2(k)\hat{D}_\mu(k)| + \frac{\Delta\hat{G}_{\mathbf{k}}}{2\hat{G}_0}(|\hat{D}_\mu(k)| + |\hat{D}_2(k)|) + a\hat{G}_{\mathbf{k}}(|\hat{D}_\mu(k)| - |\hat{D}_2(k)|) < 0. \quad (20)$$

When decreasing diffusivities, the instability first occurs for values of  $\mathbf{k}$  leading to negative values of  $\hat{G}_{\mathbf{k}}$  and for  $(|\hat{D}_\mu(k)| - |\hat{D}_2(k)|) a > 0$ . Due to the linear dependence in  $a$ , the earliest instability appears for the values of  $a$  at the extremes of its definition range, i.e., for  $a = -\Delta/(2\hat{G}_0)$  if  $|\hat{D}_2(k)| > |\hat{D}_\mu(k)|$  and for  $a = \Delta/(2\hat{G}_0)$  if  $|\hat{D}_2(k)| < |\hat{D}_\mu(k)|$ . This means that the homogeneous configurations that first become unstable are those populated by solely Lévy (when  $|\hat{D}_2(k)| > |\hat{D}_\mu(k)|$ ) or solely Brownian (when  $|\hat{D}_2(k)| < |\hat{D}_\mu(k)|$ ) walkers. The unstable mode associated to these instabilities involves only the Lévy or the Brownian population, respectively, so that the pattern that will grow from the unstable state will contain only that species. Once clusters appear in some part of the domain, arguments similar to the ones presented in Sec. 3 indicate that they will dominate the whole system. The value of  $k$  to be

used in the above expressions is the critical one,  $k_c$ , at which the instability condition (20) is first achieved, i.e.,  $k = k_B \approx 4.77901/R$  for the Brownian homogeneous background (see Table 1) should be used in  $|\hat{D}_2(k)|$ , and  $k = k_L$ , the critical wavenumber  $k_c$  for the Lévy homogeneous background, should be used in  $|\hat{D}_\mu(k)|$ . These critical wavenumbers can be read-off from Table 1 at different values of  $\mu$ .

Thus, the picture emerging from the mean-field description is the following: at large diffusion coefficients  $\kappa$  and  $\kappa_\mu$  the two types of organisms are essentially the same and coexistence occurs (until a neutral fluctuation eliminates irreversibly one of the two species). When decreasing  $\kappa$  and/or  $\kappa_\mu$ , mixing will be not so good anymore and different regions of the system may be occupied by different proportions of bug densities that satisfy the condition  $\rho_B + \rho_L = \Delta/\hat{G}_0$ . By further decreasing the diffusion coefficients (or increasing  $\Delta$  or  $R$ ), some of these regions will encounter an instability. Which is the first one to occur depends on the sign of  $|\hat{D}_2(k_B)| - |\hat{D}_\mu(k_L)| = \kappa k_B^2 - \kappa_\mu k_L^\mu$ ; it is either a pure Lévy or a pure Brownian instability, leading to a periodic pattern with periodicity fixed by  $k_B$  or  $k_L$ , respectively.

As described before, Fig. 4 shows the outcomes of the competition process, plotted in a diagram with axes  $|\hat{D}_\mu(k_L)| = \kappa_\mu k_L^\mu$  (with  $\mu = 1$ ) and  $|\hat{D}_2(k_B)| = \kappa k^2$ . The above arguments predict that the transition occurs across the main diagonal, which is sketched in the upper part of the plot. The prediction is not quantitatively accurate, but it follows qualitatively the trend of the numerically observed transition, with the proper winning state above and below it. Although rather crude, the above linear instability arguments have been adequate to describe qualitatively the outcome of the competition process. More importantly, they identify the fluxes or escape rates out of the clusters,  $|\hat{D}_\mu(k_L)|$  and  $|\hat{D}_2(k_B)|$ , correlated with cluster width, as the important parameters quantifying the competitive advantage of one species over the other, in agreement with the qualitative arguments at the end of subsection 4.1.

At this point it is clear that all the above arguments can be repeated in the case in which we have two types of Brownian random walkers differing in their diffusion coefficient  $\kappa$ , or two species of Lévy walkers characterized by different  $\mu$  or  $\kappa_\mu$ . In all these situations the prediction will be that the species with the smallest value of the  $|\hat{D}(k_c)|$ , with  $k_c$  the corresponding critical wavenumber, has a competitive advantage.

#### 4.5. Limitations of the deterministic description of the two-species system

The predictions of the previous section for the competition outcome are only qualitatively correct, as seen in Fig. 4, but this is probably more a limitation of the linear approach used than a failure of the mean-field description. More important drawbacks arise from the lack of fluctuations in Eqs. (13). As in the single-species case, this would be relevant to describe the full extinction of the whole population when  $\Delta$  approaches zero. Also, all the members of the homogeneous family in Eq. (14) are predicted to be steady states, but the deterministic treatment already identifies correctly the change in the parameter  $a$  as a neutral mode, that will fluctuate without restoring force if noise from the stochastic birth-death process is taken into account.

Competition success in our system is associated to the pattern formation process and this has been clearly traced back (Sects. 3.1 and 3.2) to the existence of *death zones* arising from the existence of a finite interaction range  $R$ . This is well described within the deterministic approach. However, when interaction range decreases so that competitive interactions become purely local, subtle interplays between competition, diffusion and fluctuations can lead to situations qualitatively different. For example Pigolotti and Benzi (2014) show that under local interactions faster mobility gives competitive advantage, a mechanism not contained in the corresponding local mean-field description.

Perhaps the most relevant deficiency of the deterministic mean-field description is that it does not capture the situation when the two species co-exist segregated in space. To describe this situation, a careful consideration of front propagation and mutual invasion processes is needed. But it can not be based only in the continuous Eqs. (13) because such study needs to take into account, in addition to the pinning of the fronts by the periodic structures, the discrete and fluctuating nature of the system. For example, a continuous deterministic description of reaction-diffusion processes with Lévy diffusion is known to predict an infinite or accelerating speed of propagating fronts (del Castillo-Negrete et al., 2003). But this speed becomes finite in the corresponding interacting particle model (Brockmann and Hufnagel, 2007) because of the discrete nature of the particles.

## 5. Conclusions and outlook

In this paper we have summarized results on the dynamics of a class of stochastic models of competing organisms, in which the individuals undergo birth and death processes modulated by competitive interactions with their neighbors, while simultaneously performing random walks of different types (Gaussian Brownian motion and Lévy flights). We have focused on the way interactions and random motions affect each other leading to spatial instabilities and extinctions.

Under appropriate conditions, competition produces particle clustering and the formation of periodic patterns. Periodicity is of the order of the interaction range  $R$ , so that it disappears in purely local interactions ( $R \rightarrow 0$ ). This process is affected by particle motion in two ways: First random walks tend to disperse the clusters and homogenize the system, thus delaying the pattern forming instability. Second, when different types or species of random walkers are allowed to compete between them, bugs that form narrower and stronger clusters get a competitive advantage, in the sense that they outcompete the others and bring them to extinction.

We have characterized numerically instabilities, patterns and transitions, and interpreted them with heuristic arguments and with integrodifferential mean-field models that neglect fluctuations. In general these continuous models provide a good description of the individual-based dynamics, in particular the existence of the pattern forming instabilities and its wavenumber. We have pointed out some deficiencies, however, such as incorrect cluster width or coexistence outcomes. These are mainly associated with the fact that arbitrarily small densities are allowed in the mean-field description, whereas in the particle system the minimum number of particles in a region is either one or zero, with no possible value in between.

The models reviewed here are extremely simplistic, and they can not be directly compared with realistic biological settings. Predation, facilitation, parasitism, and many other types of interaction occur besides competition in real ecosystems, which would need to be taken into account. Our modeling strategy should be taken as a mathematical tool that allows a detailed understanding of basic features of competitive interactions in combination with random motions. In particular it has clearly identified the relevance of *death zones* where enhanced competition occurs, and the importance of the escape rates or fluxes out of the clusters, quantified by quantities such as  $\hat{D}(k_c)$ , in shaping competitive efficiency. Despite the theoretical charac-

ter of the models we want to mention here that nonlocal competition processes have been widely discussed in the context of species competition in niche space (Barabás et al., 2012; Leimar et al., 2013) and that some observations of phenotypic clustering are in general agreement with the pattern forming instability described here (Holling, 1992; Scheffer and van Nes, 2006; Segura et al., 2013). Also, plant competition in semiarid environments provides a framework in which pattern formation by the competitive instability has been proposed (Martínez-García et al., 2013). Here individual plants are not random walkers, but seed dispersion can be described in a similar way.

Even when focusing exclusively in the competition interaction, some words should be said on the validity of the fundamental ingredient in the particle model: the basic rates in Eq. (1). In general, when modeling competition for resources, resource dynamics should be explicitly represented together with the dynamics of the consumer population (Schoener, 1974; Zaldívar et al., 2009; Ryabov and Blasius, 2011). Effective descriptions such as Eq. (1) which consider only the consumers arise in the limit in which resource dynamics is sufficiently fast (Schoener, 1974; Hernández-García et al., 2009).

Another important ingredient for the development of the clustering instability is a clear distinction between the interior and the exterior of the interaction area, so that there is a well-defined interaction range  $R$ . This leads to the existence of ‘death zones’ where particles experience enhanced competition with neighboring clusters when these are at a distance in between  $R$  and  $2R$ . We have seen that when interactions depend on distance via an interaction kernel  $G(\mathbf{x})$  the mathematical condition for a sharply defined interaction range  $R$  is the presence of negative components in the Fourier transform of the interaction kernel,  $\hat{G}_{\mathbf{k}}$ . When they are present, the death zones, and then the pattern forming instability, occur (at small mobilities).

In the context of species competition in niche space early approaches proposed Gaussian or positively-definite kernels that precluded this feature (MacArthur and Levins, 1967; May and MacArthur, 1972; Roughgarden, 1979). But later work provided more general expressions allowing it (Schoener, 1974; Abrams, 1975; Hernández-García et al., 2009; Barabás et al., 2012; Leimar et al., 2013). We refer to the last two references for recent reviews of this species-competition setting. For organisms competing in space one can envisage several mechanisms leading to a sufficiently sharp boundary for the competition range, but perhaps the simplest example arises in plant competition, because of the finite extent of the roots. The clustering instability has been reported in that case.



Many open questions remain to be addressed. In particular a fully non-linear analytic approach able to describe two-species competition and coexistence, properly taking into account particle's discrete nature that greatly affects front propagation. In the line of including more realistic features, extensions to other types of organism motion, in particular to combinations that alternate Brownian and Lévy displacements as in Thiel et al. (2012), are worth to be explored.

### **Acknowledgment**

E.H.-G. and C.L. acknowledge financial support from Spanish MINECO and FEDER through projects INTENSE@COSYP (FIS2012-30634) and ESCOLA (CTM2012-39025-C02-01). E.H. acknowledges support from the targeted financing project SF0690030s09, and from the Estonian Science Foundation grant no. 9462.

## References

- Abrams, P., 1975. Limiting similarity and the form of the competition coefficient. *Theoretical Population Biology* 8 (3), 356 – 375.
- Abrams, P., 1983. The theory of limiting similarity. *Ann. Rev. Ecol. Syst.* 14, 359–376.
- Amarasekare, P., 2003. Competitive coexistence in spatially structured environments: a synthesis. *Ecology Letters* 6 (12), 1109–1122.
- Ausloos, M., Dirickx, M. (Eds.), 2006. *The Logistic Map and the Route to Chaos*. Springer-Verlag, Berlin.
- Barabás, G., Pigolotti, S., Gyllenberg, M., Dieckmann, U., Meszéna, G., 2012. Continuous coexistence or discrete species? A new review of an old question. *Evolutionary Ecology Research* 14, 523–554.
- Benichou, O., Loverdo, C., Moreau, M., Voituriez, R., 2011. Intermittent search strategies. *Reviews of Modern Physics* 83, 81–129.
- Berestycki, H., Nadin, G., Perthame, B., Ryzhik, L., 2009. The non-local Fisher-KPP equation: travelling waves and steady states. *Nonlinearity* 22 (12), 2813–2844.
- Birch, D. A., Young, W. R., 2006. A master equation for a spatial population model with pair interactions. *Theoretical Population Biology* 70, 26.
- Bochner, S., 1937. Stable laws of probability and completely monotone functions. *Duke Math. J.* 3, 726–728.
- Britton, N., 1989. Aggregation and the competitive exclusion principle. *Journal of Theoretical Biology* 136 (1), 57 – 66.
- Brockmann, D., Hufnagel, L., 2007. Front propagation in reaction-superdiffusion dynamics: Taming Lévy flights with fluctuations. *Phys. Rev. Lett.* 98, 178301.
- Butler, T., Goldenfeld, N., 2011. Fluctuation-driven turing patterns. *Phys. Rev. E* 84, 011112.

- Cross, M. C., Hohenberg, P. C., 1993. Pattern formation outside of equilibrium. *Rev. Mod. Phys.* 65, 851–1112.
- de Jager, M., Weissing, F. J., Herman, P., Nolet, B. A., van de Koppel, J., 2011. Lévy walks evolve through interaction between movement and environmental complexity. *Science* 332, 1551–1553.
- del Castillo-Negrete, D., Carreras, B. A., Lynch, V. E., 2003. Front dynamics in reaction-diffusion systems with Lévy flights: A fractional diffusion approach. *Phys. Rev. Lett.* 91, 018302.
- Dieckmann, U., Law, R., Metz, J., 2001. *The geometry of ecological interactions: Simplifying spatial complexity.* Cambridge University Press, Cambridge.
- Dieterich, P., Klages, R., Preuss, R., Schwab, A., 2008. Anomalous dynamics of cell migration. *Proc. Natl. Acad. Sci. USA* 105, 459–463.
- Fife, P. C., 1979. *Mathematical Aspects of Reacting and Diffusing Systems.* Springer-Verlag, Berlin.
- Fort, H., Scheffer, M., van Nes, E. H., 2009. The paradox of the clumps mathematically explained. *Theoretical Ecology* 2 (3), 171–176.
- Fuentes, M. A., Kuperman, M. N., Kenkre, V. M., 2003. Nonlocal interaction effects on pattern formation in population dynamics. *Phys. Rev. Lett.* 91 (15), 158104.
- Genieys, S., Volpert, V., Auger, P., 2006. Pattern and waves for a model in population dynamics with nonlocal consumption of resources. *Mathematical Modelling of Natural Phenomena* 1, 63–80.
- Heinsalu, E., Hernández-García, E., López, C., 2010. Spatial clustering of interacting bugs: Lévy flights versus Gaussian jumps. *Europhys. Lett.* 92, 40011, erratum: *Europhys. Lett.* 95, 69902 (2011).
- Heinsalu, E., Hernández-García, E., López, C., 2012. Competitive Brownian and Lévy walkers. *Phys. Rev. E* 85, 041105.
- Heinsalu, E., Hernández-García, E., López, C., 2013. Clustering determines who survives for competing Brownian and Lévy walkers. *Phys. Rev. Lett.* 110, 258101.

- Hernández-García, E., López, C., 2004. Clustering, advection, and patterns in a model of population dynamics with neighborhood-dependent rates. *Phys. Rev. E* 70 (1), 016216.
- Hernández-García, E., López, C., 2005a. Numerical studies of an interacting particle system and its deterministic description. *Physica A* 356, 95 – 99.
- Hernández-García, E., López, C., 2005b. Birth, death and diffusion of interacting particles. *J. Phys.: Condens. Matter* 49 (17), S4263–S4274.
- Hernández-García, E., López, C., Pigolotti, S., Andersen, K. H., 2009. Species competition: coexistence, exclusion and clustering. *Phil. Trans. R. Soc. A* 367, 3183–3195.
- Holling, C. S., 1992. Cross-scale morphology, geometry, and dynamics of ecosystems. *Ecological Monographs* 62 (4), 447–502.
- James, A., Plank, M. J., Edwards, A. M., 2011. Assessing Lévy walks as models of animal foraging. *J. Royal Soc. Interface* 8, 1233–1247.
- Klages, R., Radons, G., Sokolov, I. M. (Eds.), 2008. *Anomalous Transport: Foundations and Applications*. Wiley-VCH, Weinheim.
- Klausmeier, C., Tilman, D., 2002. Spatial models of competition. In: *Competition and Coexistence*. Vol. 161 of *Ecological Studies*. Springer-Verlag, Berlin, pp. 43–78.
- Leimar, O., Doebeli, M., Dieckmann, U., 2008. Evolution of phenotypic clusters through competition and local adaptation along an environmental gradient. *Evolution* 62 (4), 807–822.
- Leimar, O., Sasaki, A., Doebeli, M., Dieckmann, U., 2013. Limiting similarity, species packing, and the shape of competition kernels. *Journal of Theoretical Biology* 339, 3 – 13.
- López, C., Hernández-García, E., 2004. Fluctuations impact on a pattern-forming model of population dynamics with non-local interactions. *Physica D* 199 (1-2), 223–234.
- López, C., Hernández-García, E., 2007a. Spatial patterns in non-locally interacting particle systems. *The European Physical Journal Special Topics* 146 (1), 37–45.

- López, C., Ramos, F., Hernández-García, E., 2007b. An absorbing phase transition from a structured active particle phase. *Journal of Physics: Condensed Matter* 19 (6), 065133.
- Lotka, A., 1932. The growth of mixed populations: two species competing for a common food supply. *J. Washington Acad. Sci.* 22, 461–469.
- MacArthur, R., Levins, R., 1967. The limiting similarity, convergence, and divergence of coexisting species. *Am. Nat.* 101 (921), 377.
- Martínez-García, R., Calabrese, J. M., Hernández-García, E., López, C., 2013. Vegetation pattern formation in semiarid systems without facilitative mechanisms. *Geophysical Research Letters* 40 (23), 6143–6147.
- Maruvka, Y. E., Shnerb, N. M., 2006. Nonlocal competition and logistic growth: Patterns, defects, and fronts. *Phys. Rev. E* 73 (1), 011903.
- Matthäus, F., Jagodič, M., Dobnikar, J., 2009. *E. coli* superdiffusion and chemotaxis—Search strategy, precision, and motility. *Biophysical Journal* 97, 946 – 957.
- Matthäus, F., Mommer, M. S., Curk, T., Dobnikar, J., 2011. On the origin and characteristics of noise-induced Lévy walks of *E. coli*. *PLoS One* 6, e18623.
- May, R., MacArthur, R. H., 1972. Niche overlap as a function of environmental variability. *Proc. Nat. Acad. Sci. USA* 69 (5), 1109–1113.
- Méndez, V., Campos, D., Bartumeus, F., 2014. *Stochastic Foundations in Movement Ecology*. Springer-Verlag, Berlin.
- Metzler, R., Klafter, J., 2000. The random walk’s guide to anomalous diffusion: A fractional dynamics approach. *Phys. Rep.* 339, 1–77.
- Murray, J. D., 2002. *Mathematical Biology I. An Introduction*, 3rd Edition. *Interdisciplinary Applied Mathematics*, vol 17. Springer, New York.
- Okubo, A., Levin, S., 2001. *Diffusion and Ecological Problems*, 2nd Edition. Springer-Verlag, New York.
- Olla, P., 2012. Demographic fluctuations in a population of anomalously diffusing individuals. *Phys. Rev. E* 85, 021125.

- Pigolotti, S., Benzi, R., 2014. Selective advantage of diffusing faster. *Phys. Rev. Lett.* 112, 188102.
- Pigolotti, S., López, C., Hernández-García, E., 2007. Species clustering in competitive Lotka-Volterra models. *Phys. Rev. Lett.* 98 (25), 258101.
- Pigolotti, S., López, C., Hernández-García, E., Andersen, K. H., 2010. How Gaussian competition leads to lumpy or uniform species distributions. *Theoretical Ecology* 3, 89–96.
- Ramos, F., López, C., Hernández-García, E., Muñoz, M. A., 2008. Crystallization and melting of bacteria colonies and Brownian bugs. *Phys. Rev. E* 77, 021102.
- Romanczuk, P., Bär, M., Ebeling, W., Lindner, B., Schimansky-Geier, L., 2012. Active Brownian particles. *Eur. Phys. J. Special Topics* 202, 1–162.
- Roughgarden, J., 1979. *Theory of Population Genetics and Evolutionary Ecology: an Introduction*. Macmillan Publishers, New York.
- Ryabov, A. B., Blasius, B., 2011. A graphical theory of competition on spatial resource gradients. *Ecology Letters* 14 (3), 220–228.
- Sasaki, A., 1997. Clumped distribution by neighbourhood competition. *Journal of Theoretical Biology* 186 (4), 415 – 430.
- Scheffer, M., van Nes, E. H., 2006. Self-organized similarity, the evolutionary emergence of groups of similar species. *Proc. Natl. Acad. Sci. USA* 103 (16), 6230–6235.
- Schoener, T. W., 1974. Some methods for calculating competition coefficients from resource-utilization spectra. *Am. Nat.* 108 (961), 332.
- Segura, A., Kruk, C., Calliari, D., Garcia-Rodriguez, F., Conde, D., Widdicombe, C. E., Fort, H., 2013. Competition drives clumpy species coexistence in estuarine phytoplankton. *Scientific Reports* 3, 1037.
- Thiel, F., Schimansky-Geier, L., Sokolov, I. M., 2012. Anomalous diffusion in run-and-tumble motion. *Phys. Rev. E* 86, 021117.

- Volterra, V., 1926. Variazioni e fluttuazioni del numero d'individui in specie animali conciventi (Variations and fluctuations of the number of individuals in animal species living together). Memoria della R. Accademia Nazionale dei Lincei, Ser. VI 2, 31–113, translated in Chapman, R. [1931] *Animal Ecology* (McGraw Hill, New York), pp. 409–448.
- Young, W. R., Roberts, A. J., Stuhne, G., 2001. Reproductive pair correlations and the clustering of organisms. *Nature* 412, 328–331.
- Zaldívar, J., Bacelar, F., Dueri, S., Marinov, D., Viaroli, P., Hernández-García, E., 2009. Modeling approach to regime shifts of primary production in shallow coastal ecosystems. *Ecological Modelling* 220 (21), 3100 – 3110.

$\mu$	$\nu_c$	$q_c = k_c R$	$\delta/R = 2\pi/q_c$
0.1	17.8039	5.11619	1.22810
0.5	34.1020	5.03951	1.24679
1.0	76.1997	4.94708	1.27008
1.5	168.726	4.85988	1.29287
2.0	370.384	4.77901	1.31475

Table 1: Critical value  $\nu_c$  such that if  $\nu > \nu_c$  the growth rate in Eq. (11) becomes positive and pattern formation occurs, for Lévy walkers of different values of  $\mu$ , and for the Gaussian case which is labeled with the value  $\mu = 2$ . The selected wavenumber  $q_c$  and the associated pattern periodicity  $\delta$  are also displayed.



## Figures

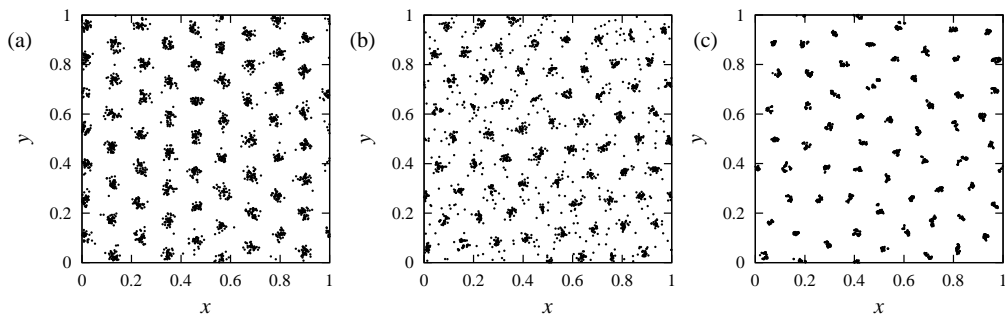


Figure 1: Snapshots of configurations of competing bugs in statistically steady states. In all panels  $r_{b0} = 1$ ,  $r_{d0} = 0.1$ , and  $R = 0.1$ . In (a) and (b) competition enters only in the birth rate, with  $\alpha = 0.02$  and  $\beta = 0$ . (c) considers competition only in the death rate,  $\alpha = 0$ ,  $\beta = 0.02$ . Motion in panels (a) and (c) is of the Gaussian type, with  $\kappa = 10^{-5}$ . Lévy flights with  $\mu = 1$  and  $\kappa_\mu = 56 \times 10^{-5}$  occur in (b).

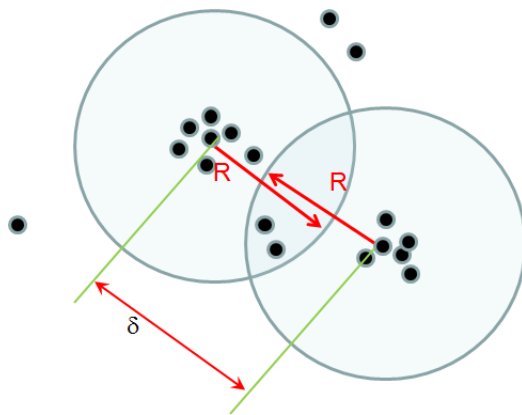


Figure 2: A sketch illustrating the mechanism of the clustering instability: two main clusters of particles are displayed, separated by a distance  $\delta$  between  $R$  and  $2R$ . The circles approximate the respective competition ranges. Particles in the intersection between the two ranges, the *death zone*, experience competition from bugs in the two clusters.

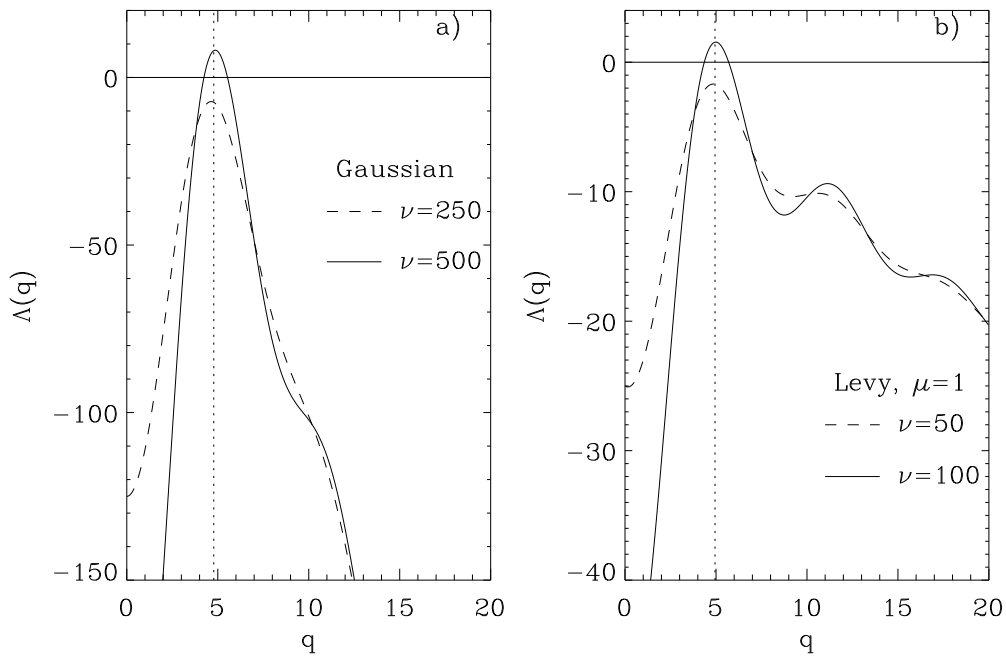


Figure 3: The linear growth rate from Eq. (11). Panel a) displays the Gaussian case (formally  $\mu = 2$  in Eq. (11)) for two values of  $\nu$ , one below and another above the cluster instability occurring at  $\nu_c = 370.384$  (see Table 1). Panel b) is for the Lévy case with  $\mu = 1$  for which  $\nu_c = 76.1997$ . In both panels the vertical dotted line indicates the critical wavenumber ( $q_c$  from Table 1) at which instability first occurs.

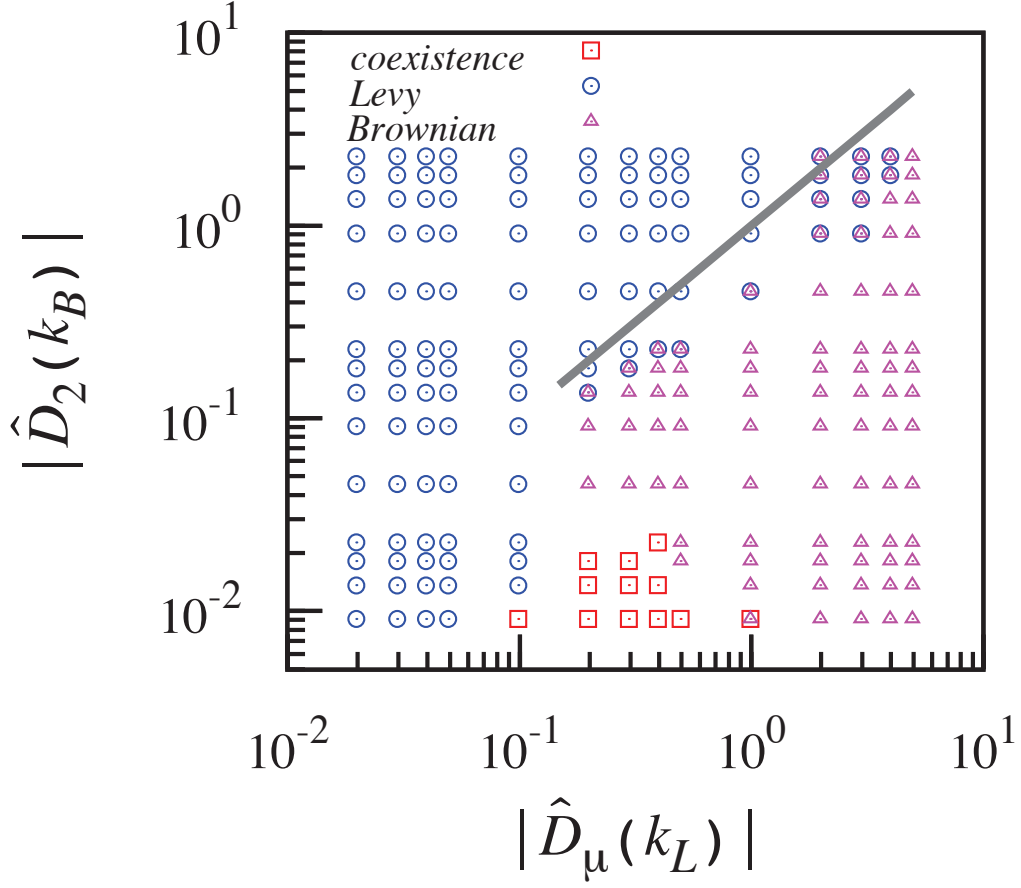


Figure 4: Outcome of competition between Brownian and Lévy walkers (with  $\mu = 1$ ) at  $r_{b0} = 1$ ,  $r_{d0} = 0.1$ ,  $R = 0.1$ ,  $\alpha = 0.02$  and  $\beta = 0$ . Symbols indicating which is the winner in the competition are displayed as a function of the quantities  $|\hat{D}_\mu(k_L)| = \kappa_\mu(q_c/R)^\mu = 49.47 \kappa_1$  for the Lévy walkers, and  $|\hat{D}_2(k_B)| = \kappa(q_c/R)^2 = 2284\kappa$  for the Brownian ones (critical wavenumber values  $q_c$  are from Table 1). Depending on the diffusivity values  $\kappa$  and  $\kappa_1$  either Brownian or Lévy walkers win, or coexistence occurs. Each point reflects the outcome of 25 realizations. Superimposed symbols indicate that individual realizations end in different states. The main diagonal sketched by the straight line is the prediction for the change in winner obtained in subsection 4.4.

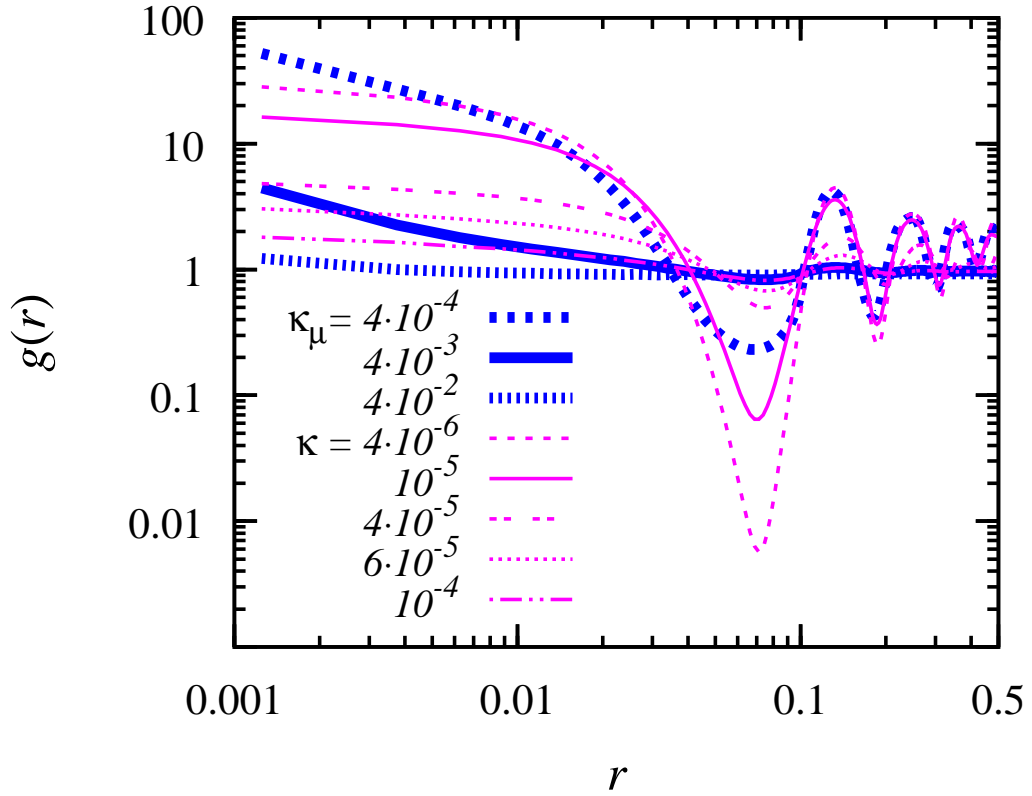


Figure 5: Radial distribution function for single-species systems consisting of Lévy walkers characterized by different values of the anomalous diffusion coefficient  $\kappa_\mu$ , with  $\mu = 1$ , or of Brownian walkers characterized by different values of diffusion coefficient  $\kappa$ . Other parameters as in Fig. 4.

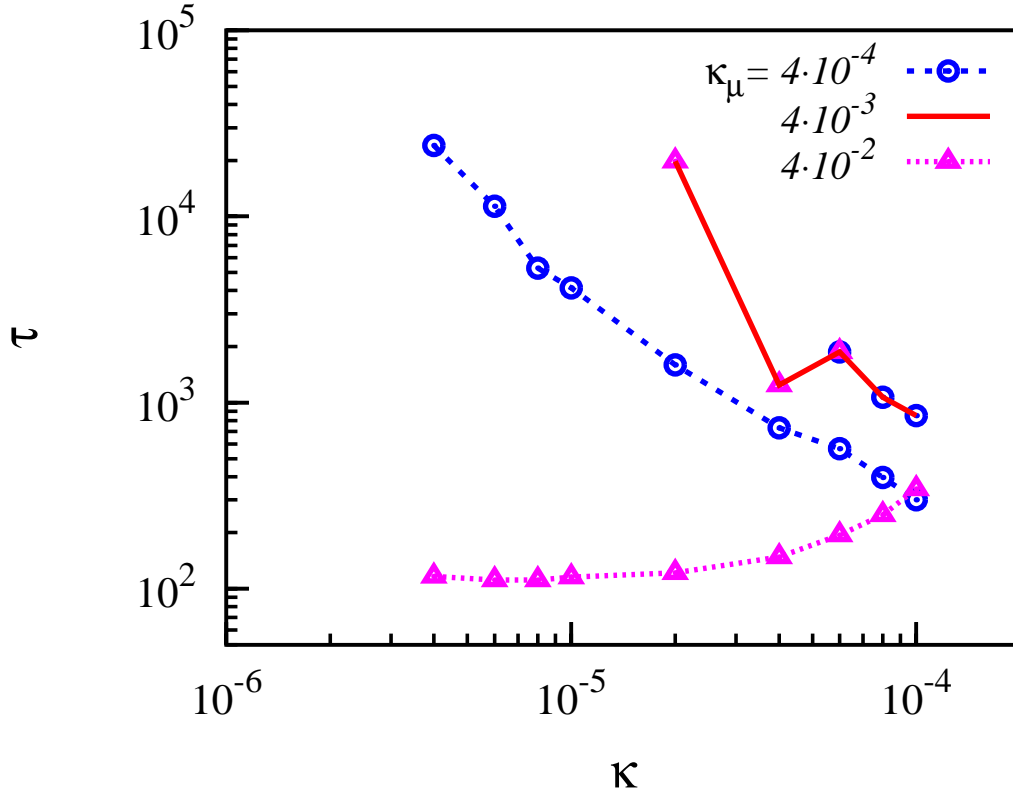


Figure 6: The fixation or extinction time,  $\tau$ , as a function of the diffusion coefficient  $\kappa$  of the Brownian walkers for three values of the anomalous diffusion coefficient,  $\kappa_\mu$ , of the Lévy walkers (with  $\mu = 1$ ). Other parameters as in Figs. 4 and 5. The symbols are the same as in Fig. 4, referring to which species survives in the competition; i.e., for  $\kappa_\mu = 4 \times 10^{-4}$  ( $|\hat{D}_\mu(k_L)| = 0.0198$  in Fig. 4) we depict the extinction time of Brownian walkers (Lévy walkers win the competition) and for  $\kappa_\mu = 4 \times 10^{-2}$  ( $|\hat{D}_\mu(k_L)| = 1.98$ ) the extinction time of Lévy walkers (Brownian walkers win the competition). For the intermediate value  $\kappa_\mu = 4 \times 10^{-3}$  ( $|\hat{D}_\mu(k_L)| = 0.198$ ) we observe the two types of outcome, as indicated by the different symbols. The results are obtained by averaging over 25 realizations.